High Frequency, Low Force Dynamometer for Micro-Milling Force Measurement

David Burton, G. Scott Duncan, John C. Ziegert, Tony L. Schmitz
University of Florida, Gainesville, FL 32611

Introduction

The need for miniature components in such applications as biomedical, aerospace, electronics, and mold production has led to the development of micro-milling processes that are characterized by high spindle speeds (up to 500,000 rpm) and low cutting force magnitudes (<1 N). Due to these high spindle speeds, the tooth passing frequency, and, therefore, the fundamental cutting force frequency, can reach 16 kHz for a two tooth cutter. Harmonics of the fundamental cutting force frequency are also present for partial radial immersion cuts. Many researchers have attempted to model cutting forces during the micro-milling process [1-3]; however, to better understand the micro-milling process and validate these cutting force models, there is a need to quantify cutting forces at high frequencies and low cutting force amplitudes.

Commercially-available dynamometers typically specify a bandwidth below the first natural frequency of the dynamometer structure (typically 1 kHz to 3 kHz in practice). Operation in this range enables the actual force to be determined by multiplying the time-domain dynamometer signal by a calibration constant. For operation outside this range, it is necessary to multiply the sensor signal (transformed to the frequency domain) by the inverted dynamometer frequency response function (FRF) to remove the influence of the dynamometer dynamics from the recorded signal [4]. However, this approach is limited because the frequency response magnitude is generally so small at higher frequencies that it is not possible to recover a valid force signal due to a poor signal-to-noise ratio. Additional difficulties in measuring low cutting forces at high frequencies include: 1) the requirement of a high resolution measurement device with a very large bandwidth, 2) a method to excite the structure with a known input at all frequencies of interest to determine the FRF of the dynamometer system, and 3) a dynamometer system design capable of limiting the effect of forces in coordinates other than the coordinate of interest.

This paper presents a concept for a dynamometer designed to operate within a frequency range of 10 kHz to 16 kHz while measuring cutting forces less than 1 N. The design is based on two coupled, single degree-of-freedom (SDOF) flexures that interact to produce vibration modes at the edge of the bandwidth of interest. These modes produce a FRF within the desired frequency band that has a magnified response and nearly constant value between modes. The workpiece is mounted to the first of the two flexures while a precision accelerometer with a frequency range up to 20 kHz is mounted to the second flexure. To limit the effect of additional structural modes, finite element analysis (FEA) is used to optimize the flexure design by forcing the natural frequencies of additional modes above the bandwidth of interest. To validate the dynamometer design prior to manufacture, an uncertainty analysis is performed.

System Model

The flexure design goal was to include only two vibration modes below 16 kHz, specifically, linear translation of both the workpiece and accelerometer flexures. The system was initially modeled as a 2DOF lumped mass, spring, damper system with stiffness determined from flexure theory [5] and mass and damping characteristics determined from flexure geometry and material properties. To refine the model, Ansys Workbench 8.0 [6] was selected as FEA software. The final 2DOF flexure design is shown in Fig. 1 along with the desired first two system modes (at 9628 Hz and 17688 Hz).

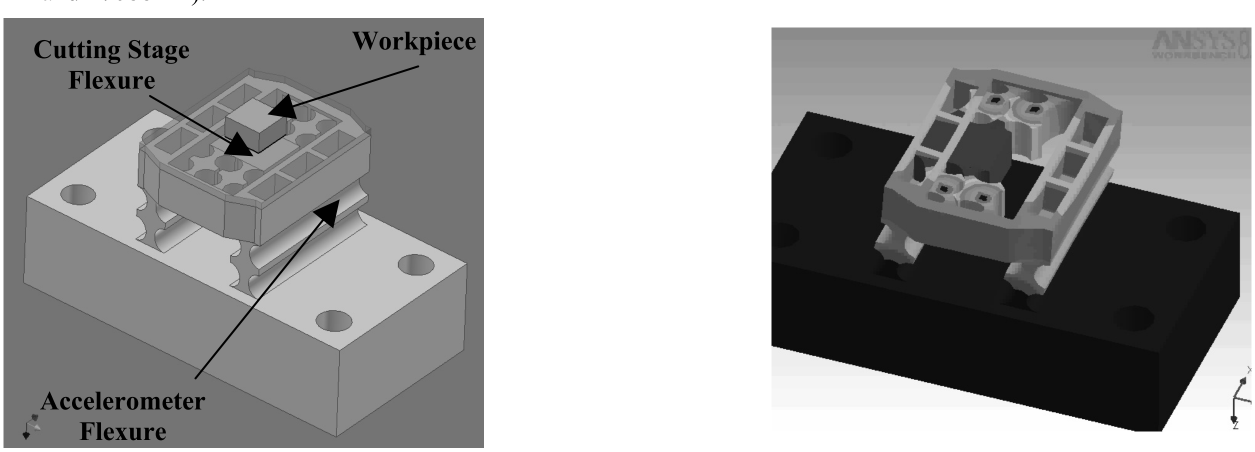

Figure 1: 2DOF flexure design; the workpiece flexure is carried on the accelerometer flexure

The critical flexure parameters are shown in Fig. 2 with the corresponding values provided in Table 1. Due to its high strength to density ratio, the flexure material was selected as tungsten carbide. The FEA-predicted FRF of the 2DOF flexure design is displayed in Fig. 3. As seen in the figure, the FRF has a nearly constant value in the frequency bandwidth of interest, between the 9628 Hz and 17688 Hz modes.

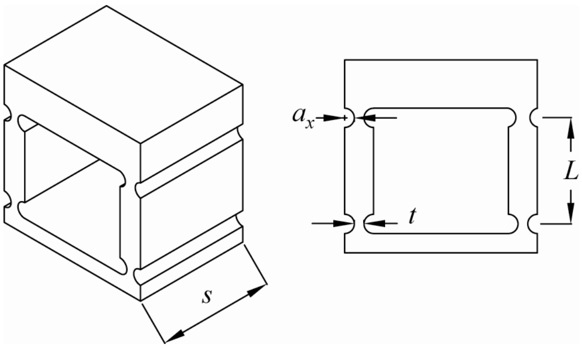

Figure 2: Flexure design parameters

Parameters	Accelerometer Flexure	Workpiece Flexure
a_x (mm)	1.75	1.75
s (mm)	29.00	5.00
t (mm)	1.50	1.00
L (mm)	4.50	4.50

Table 1: Flexure geometry values

Uncertainty Analysis

The uncertainty analysis developed in this section provides 95% confidence intervals on the measured cutting force. The uncertainty analysis is dependent on the cutting force signal; therefore, simulation [7] is used to generate two input signal cases for a 420 krpm spindle speed using a two tooth cutter: 1) a slotting cut, and 2) a 50 percent radial immersion cut. To convert the simulated cutting force signal to an acceleration signal, the force signal is Fourier transformed to the frequency domain, multiplied by the acceleration to force frequency response of the dynamometer system (produced from FEA), and inverse Fourier transformed back to the time domain. Chip loads were selected to generate cutting force amplitudes that approximated previously predicted and measured values for micro-milling operations [1-3]. Figure 4 displays the input cutting force signal for both uncertainty analysis cases.

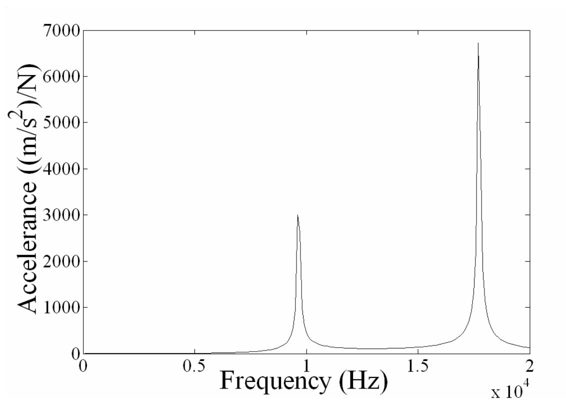

Figure 3: Model FRF results

Uncertainty contributors occur on each time sample of the acceleration signal in the time domain and on each point of the measured FRF in the frequency domain. The uncertainty contributors in the time domain include: (1) accelerometer resolution, (2) electrical noise and external vibration, and (3) contributions from additional system modes, and the uncertainty contributors in the frequency domain include: (1) measurement variation, (2) ambient temperature, (3) dynamic changes due to material removal, and (4) dimensional and material variation. Each of the contributors is assumed to have a uniform distribution across a selected range. For the accelerometer resolution, the distribution range (0.04 m/s^2) was specified as twice the resolution of the device and the electrical noise and external vibration range (0.3 m/s^2) was determined by measuring the signal of an accelerometer mounted to a tombstone while a spindle rotated and completed linear moves. The range of the additional system modes was determined by multiplying a Fourier transformed cutting signal for the direction (y) orthogonal to the desired force measurement direction (x) by an FEA-predicted FRF for two cases: 1) the x direction flexure motion to the y

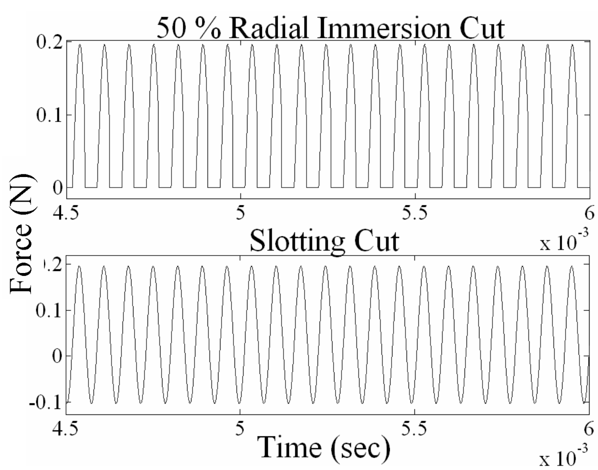

Figure 4: Cutting force signals

direction input force at the center of the work piece; and 2) the x direction flexure motion to the y direction input force at the edge of the work piece. The frequency domain uncertainty was then inverse Fourier transformed to the time domain and applied to each time sample. For the measurement variation in the frequency domain, the distribution range was set using the statistical variation determined from previous modal testing (2% of the measured FRF). The temperature distribution range was determined by subtracting the FEA-predicted FRF at 20 °C from FRF at 25 °C. The geometric and material variation properties included the dimension of the notch radius, the modulus of elasticity, Poisson's ratio, and material damping. The FEA model was used to produce FRFs for ±5% of the nominal values for each of the properties and the distribution range was set by subtracting the low value FRF from the high value FRF. Finally, the material removal distribution range was determined by subtracting the FEA-predicted FRF with 10% of the work piece material removed from the FRF with a complete work piece. The individual time domain uncertainties were joined to create a combined uncertainty as shown in Eq. (1), where σ specifies the standard deviation and *n* is the total number of uncertainty contributors. The procedure was repeated for the frequency domain uncertainties. The standard deviation of a uniform distribution was calculated from Eq. (2) [8].

$$\sigma^2_{combined} = \sigma_1^2 + \sigma_2^2 + \ldots + \sigma_n^2 \qquad (1)$$

$$\sigma^2 = \frac{Range^2}{12} \qquad (2)$$

To account for uncertainties in both the time and frequency domains, a Monte Carlo simulation was completed to generate the 95% confidence intervals around the x-direction cutting force signal. The following steps were used to determine this result: 1) the acceleration signal, based on the initial cutting force signal, was multiplied by a randomly generated value based on the combined standard deviation of the time domain uncertainties; 2) the new acceleration signal was Fourier transformed to the frequency domain; 3) the FRF of the dynamometer (produced by FEA) was multiplied by a randomly generated value based on the combined standard deviation of the frequency domain uncertainties; 4) the new acceleration signal was multiplied by the inverse of the new dynamometer FRF to produce a cutting force signal in the frequency domain; and 5) the cutting force signal was inverse Fourier transformed back to the time domain. These steps were repeated 1000 times to determine a mean cutting force signal and standard deviation in the time domain. To create 95% confidence intervals, two times the standard deviation was added to the mean of the cutting force signal at each time sample. The original cutting force signal, the Monte Carlo mean, and the 95% confidence intervals are shown in Fig. 5 for the slotting cut and Fig. 6 for the 50 percent radial immersion cut.

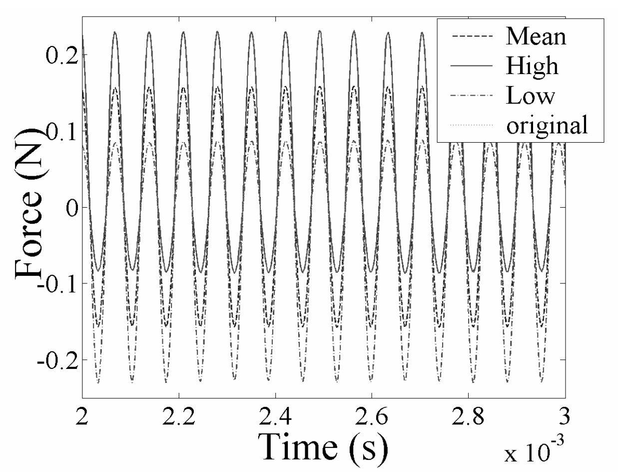

Figure 5: 95 percent confidence intervals for slotting

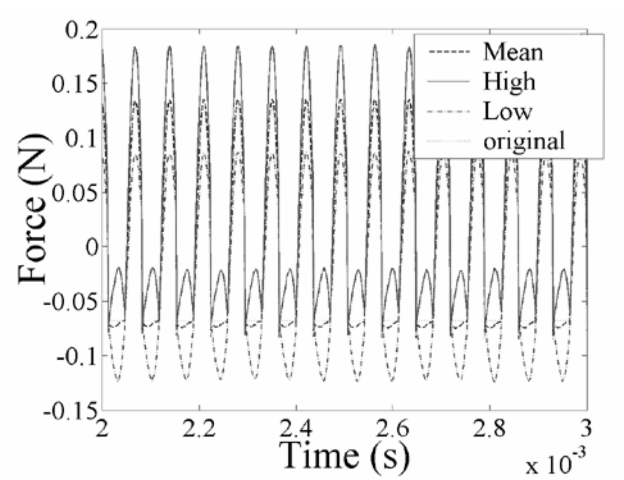

Figure 6: 95 percent confidence intervals for 50 percent radial immersion cut

A large percentage of the uncertainty is due to material property and dimensional variation. This is very important in producing a dynamometer that will operate in the specified range; however, these properties will be captured in the measured FRF of the actual dynamometer system, effectively removing their uncertainty from the measured cutting force signal. As an approximation to the final 95% confidence intervals of an actual dynamometer, the confidence intervals for a slotting cut and 50 percent radial immersion cut with material property and dimensional uncertainties removed are shown in Figs. 7 and 8, respectively.

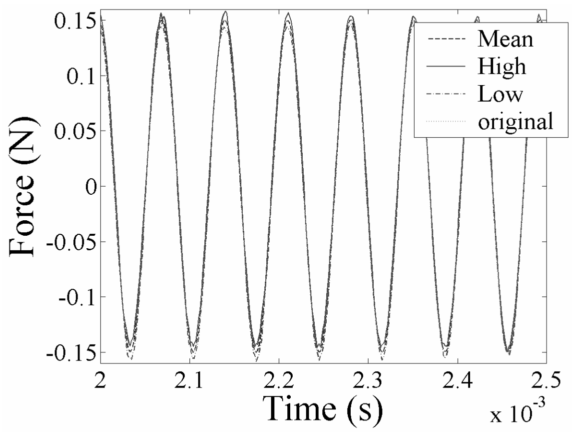

Figure 7: 95 percent confidence intervals for slotting cut excluding material property and dimensional uncertainties

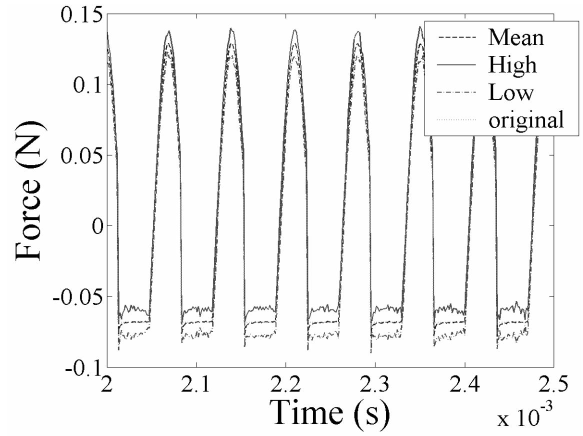

Figure 8: 95 percent confidence intervals for 50 percent radial immersion cut excluding material property and dimensional uncertainties

Measurement and Excitation Issues

Determination of the FRF of the dynamometer system requires exciting the structure across the desired bandwidth, 10 to 16 kHz, and providing a measurement device that is capable of sensing the response across the same bandwidth. To verify that excitation is possible for this bandwidth, testing was performed using a small piezoelectric impact hammer with a hard, steel tip on a hard surface. The time response of the hammer impact was Fourier transformed to the frequency domain and the excitation bandwidth was approximately 20 kHz. The dynamometer system accelerometer with a 20 kHz bandwidth can be used to measure the response. To validate the dynamometer system, a piezoelectric shaker in conjunction with an integral high frequency force transducer is capable of exciting the dynamometer system with a bandwidth of 20 kHz with a known input. In this manner, the operation of the dynamometer output can be verified and calibrated to a known input.

Conclusions

A 2DOF, flexure based design for a high frequency, low force dynamometer to measure micro-milling cutting forces was investigated using analytical and FEA techniques. The dynamometer design limited the effect of unwanted structural modes and provided an acceptable resolution-to-response ratio for the sensing device. An uncertainty analysis, based on Monte Carlo techniques, was also performed. The results of the analysis predict that the proposed dynamometer will be capable of providing cutting force measurements with acceptable uncertainty.

References

[1] Dow, T., Miller, E., Garrard, K., 2004, “Tool Force and Deflection Compensation for Small Milling Tools”, Precision Engineering, **28**, pp. 31-45.

[2] Bao, W., Tansel, I., 2000, “Modeling Micro-End-Milling Operations. Part I: Analytical Cutting Force Model”, International Journal of Machine Tools and Manufacture, **40**, pp. 2155-2173.

[3] Rahman, M., Kumar, S., Prakash, J., 2001, “Micro Milling of Pure Copper”, Journal of Materials Processing Technology, **116**, pp. 39-43.

[4] Tounsi, N., Otho, A., 2000, “Dynamic Cutting Force Measuring”, International Journal of Machine Tools and Manufacture, **40**, pp. 1157-1170.

[5] Smith, S., 2000, Flexure Elements of Elastic Mechanisms, Gordon and Breach Science Publishers, Amsterdam, The Netherlands.

[6] Ansys, Inc., 2003, Ansys 8.0 Workbench: Finite Element Analysis Software, Canonsburg, Pennsylvania.

[7] Smith, S., Tlusty, J., 1991, “An Overview of Modeling and Simulation of the Milling Process”, ASME Journal of Engineering for Industry, **113**, pp. 169-175.

[8] Wackerly, D., Mendenhall, W., Scheaffer, R., 2002, Mathematical Statistics with Applications, Duxbury, Pacific Grove, CA.